Optics Letters

Circular dichroism of a tilted U-shaped nanostructure

TianKun Wang, Tong Fu, Yuyan Chen, and Zhongyue Zhang*

School of Physics and Information Technology, Shaanxi Normal University, Xi'an 710062, China
**Corresponding author: zyzhang@snnu.edu.cn*

Received 31 May 2017; revised 21 June 2017; accepted 21 June 2017; posted 27 June 2017 (Doc. ID 297156); published 14 July 2017

The circular dichroism (CD) effect plays an important role in biological detection, analytical chemistry, and plasmonic sensing. Tilted 3D structures can generate CD signals under normal illumination. However, fabricating tilted 3D structures is complex and expensive. In this study, we fabricate a tilted U-shaped nanostructure (TUSN) on a polystyrene (PS) nanosphere through the glancing angle deposition method. One branch of the U-shaped nanostructure is tilted by raising a sheet of SiO_2 on the PS nanosphere. And the CD signal of the TUSN is enhanced because the phase difference increases with increasing thickness of the SiO_2 sheet. This work proposes a method for fabricating tilted nanostructures and elucidates the mechanism of the CD effect for future research.

OCIS codes: (310.1860) Deposition and fabrication; (310.6628) Subwavelength structures, nanostructures; (240.6680) Surface plasmons; (160.1585) Chiral media; (220.4241) Nanostructure fabrication.

https://doi.org/10.1364/OL.42.002842

Chirality has attracted significant research attention in different fields due to its essential role in nature. A chiral structure cannot be superposed on its mirror image and elicits different responses under left circularly polarized (LCP) and right circularly polarized (RCP) light [1–4]. Chiral structures under LCP and RCP light may induce interesting phenomena, such as circular dichroism (CD) [4] and optical rotatory dispersion [5]. Many chiral structures have been designed to obtain the CD effect, which is widely applied to many fields, such as biological monitoring, analytical chemistry, and plasmonic sensing [6–8].

The chiral structure in the natural world is generally 3D, such as DNA and protein. For artificial metal 3D structures, such as layer-by-layer structures and helix [9–13], the CD effect can be detected under normal illumination. The evident CD effect of layer-by-layer structures originates from electric dipoles with different orientations on different layers. For the helix, the ring current on the helix can generate magnetic dipoles. The CD effect occurs when the angle between two electric dipoles is less than or greater than 90°. Normal illumination can also cause the CD effects of planar chiral structures [14–16]. The CD signal of planar chiral structures is due to the chiral symmetry and induces small-scale defects. And the CD effect also occurs when electric resonances are not parallel and there is phase difference. Planar achiral structures cannot generate the CD effect under normal illumination [17]. In addition to electric and magnetic dipoles, the CD effect can also be interpreted by Born–Kuhn configurations [18,19].

Several experimental methods are generally utilized to fabricate nanometal structures that can generate CD effects; these methods include electron beam lithography (EBL), laser writing, and self-assembly method. EBL is used to fabricate 3D structures on the plane and layer-by-layer structures, but it is difficult to apply to fabricate the tilted structures. EBL is complex and time consuming, and the effective area of the template made through this method is limited [20,21]. Laser writing can also be used to fabricate 3D structure [22]; the size of the sample fabricated through laser writing not only depends on the wavelength of light but also on scanning accuracy and laser focal spot diameter. Compared with these two methods, self-assembly is regarded as more efficient for preparing chiral nanostructures for large-scale application; this method is cheap, fast, and tunable [23,24]. However, this method is restricted to simple geometries, usually nanospheres and nanorods. Glancing angle deposition (GLAD) is used to generate simple plasmonic nanostructures with a large area [25]; this method comprises several simple deposition steps rather than complex laser writing and EBL technology. The formed tilted 3D structures can induce the generation of CD signals [26,27]. Fabricating an experimentally tilted structure through EBL, laser writing, and the self-assembly method is difficult. Previous studies on the CD of tilted structures involve numerical calculations [26,27,28].

In this study, we fabricate a silver tilted U-shaped nanostructure (TUSN) through GLAD on a self-assembled polystyrene (PS) sphere monolayer. A branch of the silver U-shaped nanostructure is raised by a slice of SiO_2 sheet. Experimental results show five obvious CD modes in the visible and near-IR regions of the titled U-shaped nanostructure. The CD intensity of the TUSN is enhanced with increasing SiO_2 thickness, that is, the U-shaped nanostructure becomes more tilted, and the CD signal is larger. The simulation results are consistent with the experimental data. Moreover, the CD effect could be due to the surface charge distributions of the Ag sheets. This study not only provides a concise method for fabricating tilted chiral

nanostructures but also contributes to elucidating the physical mechanism of CD.

The main mechanism of GLAD is the geometric shadowing effect, namely, the evaporated material cannot be deposited on shadow areas in the vaporing direction [25,27–31], and the self-assembly of monolayer PS nanospheres on glass substrates can generate the geometric shadowing effect. The fabrication of the TUSN starts with the self-assembly of monolayer PS nanospheres on glass substrates. Here we choose the PS sphere with a diameter $d = 380$ nm to pave on the glass sheet. The progress of fabricating the TUSN on a template needs four steps, as shown in Fig. 1(a). In the first step, Ag is deposited on one side of the monolayer at a fixed polar angle $\varphi = 0°$, and the thickness is set as 30 nm. In the second step, SiO_2 is deposited on the other side of the monolayer at a fixed polar angle $\varphi = 180°$, and the thickness is set as 60 nm. Then, in the third step, at the same polar angle $\varphi = 180°$, 30 nm Ag is deposited on the SiO_2 sheet. In the last step, the substrate is clockwise (anticlockwise) rotated an angle of $\Delta\varphi = 90°$, namely, the polar angle at 90° (270°), Ag is deposited 30 nm, the left-hand TUSN (L-TUSN) [right-hand TUSN (R-TUSN)] is fabricated, as shown in Fig. 1(b). Here φ is defined as polar angle. θ is the angle of substrate azimuthal orientation, it is defined as the angle between the normal of the sample plane and the direction of vapor. And the azimuthal angle θ is fixed at 86° in all steps. The actual thickness is about half of the value of thickness in the electron beam vapor after a lot of experiments and measurement verification [18]. And the whole size of the sample we made is 1.1*2.4 cm.

Figure 2(a) shows the scanning electron microscope (SEM) image of the R-TUSN from the top view. It is easy to distinguish the Ag deposited on the PS sphere and SiO_2 sheet through the smoothness and flatness of the surface of Ag. The Ag on the left part of the PS sphere is smooth and flat, but the Ag on the right part of the PS sphere is cobbly since the Ag is deposited on the SiO_2 sheet. Figures 2(b) and 2(c) show the transmission electron microscope (TEM) images of the R-TUSN, the view of observation and the schematic are shown in the top of the images. It can be seen from the figures that the Ag deposited in the last step is tilted [Fig. 2(b)] and the two branches of the U-shaped structure are in different planes and separated by SiO_2 [Fig. 2(c)]. All of those images can demonstrate that the U-shaped structure is tilted.

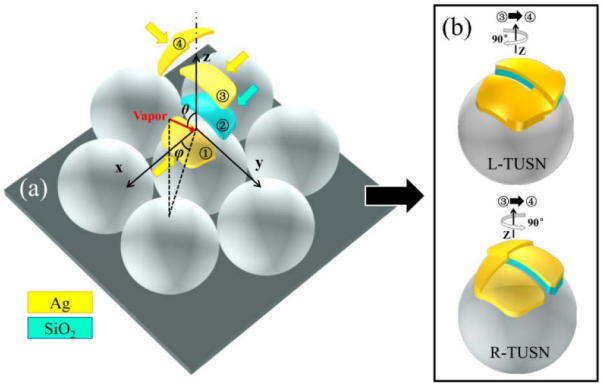

Fig. 1. (a) Fabrication steps of U-shaped nanostructures on the PS sphere. The yellow domain is Ag, and the lake blue domain is SiO_2. (b) The schematics of L-TUSN and the R-TUSN.

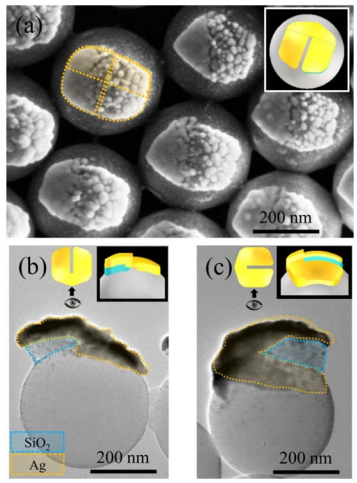

Fig. 2. (a) SEM image of the top view of R-TUSN. (b), (c) TEM images of R-TUSN from different observation views.

Chirascan (Applied Photophysics Ltd.) is used to record the absorbance and CD spectrum. Figure 3(a) shows the absorbance of the L-TUSN (red line) and the R-TUSN (blue line) with 15 nm thick Ag and 30 nm thick SiO_2 under unpolarized light illumination. The black line in Fig. 3(a) represents the absorbance of the PS nanosphere on the glass substrate. All three absorbance spectra show a peak at around $\lambda = 520$ nm, which is due to the first diffracted order of 2D close-packed monolayer arrays [32] and marked as "PS."

Figure 3(b) shows the CD spectrum and g-factor (the g-factor is defined as $g = \Delta A/A$) of the R-TUSN with 30 nm thick SiO_2. Five resonance modes are marked as I, II, III, IV, and V and are located at $\lambda_I = 865$ nm, $\lambda_{II} = 535$ nm, $\lambda_{III} = 450$ nm, $\lambda_{VI} = 395$ nm, and $\lambda_V = 330$ nm, respectively.

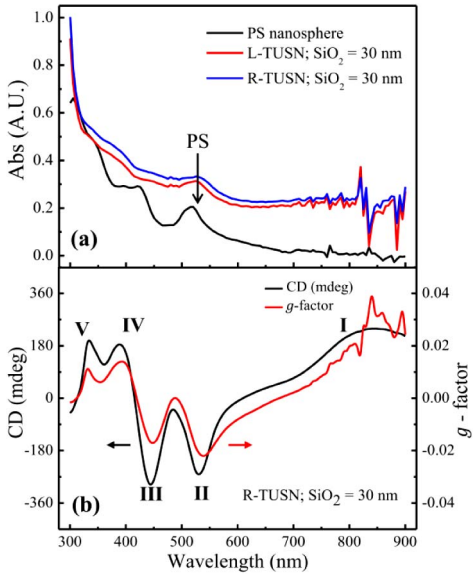

Fig. 3. (a) Absorbance of L-TUSN (red line) and R-TUSN (blue line) under the unpolarized light illumination, the black line is the absorbance of PS nanosphere. (b) The CD spectrum and g-factor of R-TUSN in experiment.

The CD spectrum is interfered by linear dichroism (LD) through Chirascan (Applied Photophysics Ltd.), which is due to the differences in absorbance caused by anisotropy of the sample [33] (SI of [18]). The sample was rotated at different polar angles (φ) along the z-axis to exclude the influence of LD [Fig. 1(a)]. Figure 4(a) shows the CD spectra of the R-TUSN with 30 nm thick SiO_2 at different φ values. When the sample is rotated, the intensities of the five modes remain almost constant; this finding indicates that LD has little effect on the received CD signal. However, for the CD signal of $SiO_2 = 0$ nm, the influence of LD cannot be ignored since the CD signal is almost zero [as the black line in Fig. 4(b)]. Figure 4(b) shows the CD spectra of the R-TUSN and L-TUSN with SiO_2 of different thicknesses. The CD effect should be zero when the thickness of SiO_2 is 0 nm if we do not consider the effect of LD. With increasing SiO_2 thickness, the intensity of the CD effect increases. Hence, the U-shaped nanostructure becomes more tilted and the CD effect becomes larger. Moreover, almost no CD effect is observed when the two branches of the U-shaped nanostructure are in the same plane.

The finite element method (radio frequency model COMSOL Multiphysics) is used to simulate the optical properties of the TUSN. The refractive index of air and SiO_2 are regarded as 1 and 1.45, respectively. The frequency-dependent permittivity of silver is referred from [34]. For the simplification, the increase of thickness of Ag and SiO_2 is regarded as a linear increase with the increase of vapor time [31]. For the hexagonal honeycomb periodic structure, there are three periodic boundaries. Circularly polarized light normally irradiates on the port, which is defined as T_{++} (RCP) and T_{--}(LCP) in the setting of COMSOL Multiphysics. The perfectly matched layers are applied at the top and bottom of the computational domain for absorbing light, which pass through the ports. Transmittance is defined as $T = P_{\text{out}}/P_{\text{in}}$, which is the ratio of output power to incident power, and the CD effect is defined as the difference of absorbance of RCP and LCP, that is, $\Delta A = A_{++} - A_{--}$, and $A = 1 - T - R$ (the R of TUSN is the same under LCP and RCP) in the siting of COMSOL, so CD can be defined as $\Delta T = T_{++} - T_{--}$ [3].

The schematic diagram of the R-TUSN is simplified in COMSOL Multiphysics to understand the mechanism of the CD effect and shown in Fig. 5(a). The geometric parameters of the R-TUSN are acquired by SEM and TEM images (Fig. 2). After the survey and measurement of the SEM images of the R-TUSN, the final geometric parameters are obtained using the average of the measured values of a large number of structures, namely, calculation results indicate the effect of a particular kind of tilted U-shaped structure. As shown in Fig. 5(b), the thickness of Ag and SiO_2 are $d_1 = 15$ nm and $d_2 = 30$ nm, respectively; the width and length of the branch of the U-shape are $w = 105$ nm and $l_1 = 205$ nm, respectively; and the length of the Ag in the final step is $l_2 = 130$ nm. And the period is an outer hexagon with a radius of 190 nm ($P_l = 220$ nm). Figure 5(c) is the CD spectrum and g-factor of the R-TUSN in simulation (CD spectrum and g-factor of the R-TUSN with the SiO_2 substrate has similar results). Because of the varietal arrays of the layout of the PS nanosphere, variations in the size and shape of the sample, and the thickness of the Ag sheet on the PS sphere is not uniform, which results in a shifty aspect ratio. And the offsets for peaks in Fig. 5(c) are due to the aspect ratio with parameters set in numerical calculation. And the simulation amplification is larger than that of the experimental one because of the cancellation effect caused by the random orientation of the PS array in the experiment [18]. But, it can be seen that there are also five modes in simulation named i, ii, iii, iv, and v. And in the simulation, the unit of CD intensity is a percentage since the CD is defined as the difference between the transmission rates in COMSOL.

Figure 6 shows the charge distribution of the R-TUSN with 30 nm thick SiO_2 under RCP illumination at resonant wavelengths. In order to conveniently analyze those five modes, the R-TUSN is regarded as being made up of four parts, which are named A, B, C, and D [Fig. 6(a)]. Specifically, at $\lambda_i = 650$ nm, the charge on parts A and B form the electric dipole $P_{i\text{-}AB}$, and the path of $P_{i\text{-}AB}$ is the longest path in the entire R-TUSN structure; the charge on part D forms the electric dipole $P_{i\text{-}D}$ [as shown in Fig. 6(b)]. And the $P_{i\text{-}AB}$ and $P_{i\text{-}D}$ form an antibonding mode. The $P_{i\text{-}AB}$ in the upper layer needs to rotate anticlockwise to be parallel to the lower layer $P_{i\text{-}D}$, as shown by the red dotted arrow in Fig. 6(b). It has a positive effect on RCP, so the CD sign is positive [18]. At $\lambda_{\text{ii}} = 620$ nm, the

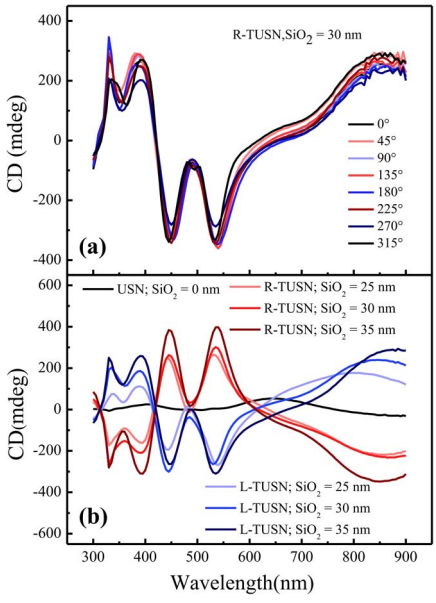

Fig. 4. (a) Method of eliminating the disturbance of linear dichroism (LD). (b) The CD spectrum of enantiomer results of different thickness of SiO_2 in experiment.

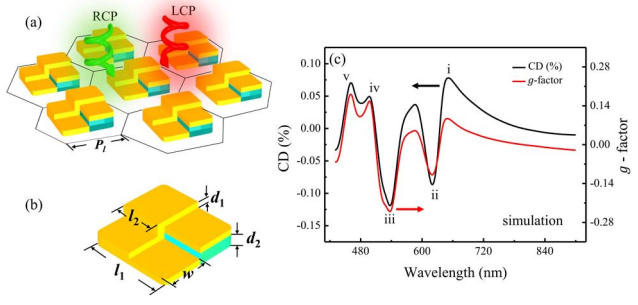

Fig. 5. (a), (b) R-TUSN calculated in COMSOL Multiphysics. The yellow domain is Ag, and the lake blue domain is SiO_2. (c) The CD spectrum and g-factor of R-TUSN of simulation.

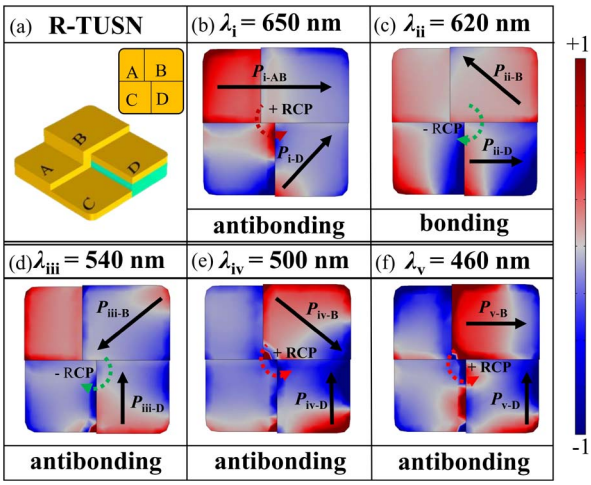

Fig. 6. Resonant modes that formed by dipole electron oscillation of surface charge on different parts of R-TUSN, and the red and green dotted arrows indicate the positive and negative effect on RCP.

charge on part B forms the electric dipole $P_{ii\text{–}B}$, and the charge on part D forms the electric dipole $P_{ii\text{–}D}$; $P_{ii\text{–}B}$ and $P_{ii\text{–}D}$ form a bonding mode, as shown in Fig. 6(c). The $P_{ii\text{–}B}$ in the upper layer needs to rotate clockwise to be parallel to the lower layer $P_{ii\text{–}D}$, as shown by the green dotted arrow in Fig. 6(c). It has a negative effect on RCP, so the CD sign is negative. Similarly, at λ_{ii} = 540 nm, $P_{iii\text{–}B}$ on part B and $P_{iii\text{–}D}$ on part D form an antibonding mode, as shown in Fig. 6(d), and it has a negative effect on RCP. At λ_{iv} = 500 nm and λ_v = 460 nm both the $P_{iv\text{–}B}$ and $P_{iv\text{–}D}$ and the $P_{v\text{–}B}$ and $P_{v\text{–}D}$ form an antibonding mode, and it has a positive effect on RCP. With increasing SiO_2 thickness, the altitude intercept of different parts of the U-shaped nanostructure increases, thereby increasing the phase difference. Thus, the CD effect is enhanced [16].

We proposed a method for fabricating silver tilted U-shaped nanostructures through GLAD to generate the CD effect. Compared to other methods mentioned in this Letter, this method requires a number of simple deposition steps on existing templates and is simple and convenient to use for controlling the tilt degree. The CD mechanism of the TUSN can be illustrated by the Born–Kuhn configurations, which are formed by effective dipole electron oscillation on different parts of the structure. The CD effect is enhanced because the phase difference increases with increasing SiO_2 thickness. This study provides a concise method for fabricating tilted structures. The proposed method is appropriate not only for GLAD but also for application to other physical deposition experiments. In addition, the method that uses simple steps to obtain relatively complex structures is a significant experiment thought, and thus exhibits potential for future studies in diverse fields.

Funding. National Natural Science Foundation of China (NSFC) (61575117); Fundamental Research Funds for the Central Universities of Ministry of Education of China (GK201601008); Fundamental Research Funds for the Central Universities (2016CSZ013).

REFERENCES

1. S. M. Kelly, T. M. Jess, and N. C. Price, Biochim. Biophys. Acta, Proteins Proteomics **1751**, 119 (2005).
2. M. Takezaki and Y. Kito, Nature **215**, 1197 (1967).
3. F. Zhu, X. Li, Y. Li, M. Yan, and S. Liu, Anal. Chem. **87**, 357 (2014).
4. M. Hentschel, L. Wu, M. Schäferling, P. Bai, E. P. Li, and H. Giessent, ACS Nano **6**, 10355 (2012).
5. M. Decker, M. Ruther, C. E. Kriegler, J. Zhou, C. M. Soukoulis, S. Linden, and M. Wegener, Opt. Lett. **34**, 2501 (2009).
6. A. V. Kildishev, A. Boltasseva, and V. M. Shalaev, Science **339**, 1232009 (2013).
7. J. B. Pendry, Science **306**, 1353 (2004).
8. J. K. Gansel, M. Thiel, M. S. Rill, M. Decker, K. Bade, V. Saile, and M. Wegener, Science **325**, 1513 (2009).
9. J. K. Gansel, M. Wegener, S. Burger, and S. Linden, Opt. Express **18**, 1059 (2010).
10. M. V. Gorkunov, A. A. Ezhov, V. V. Artemov, O. Y. Rogov, and S. G. Yudin, Appl. Phys. Lett. **104**, 221102 (2014).
11. M. Hentschel, M. Schäferling, T. Weiss, N. Liu, and H. Giessen, Nano Lett. **12**, 2542 (2012).
12. L. Wu, Z. Yang, Y. Cheng, Z. Lu, P. Zhang, M. Zhao, and J. Duan, Opt. Express **21**, 5239 (2013).
13. T. Cao, L. Zhang, R. E. Simpson, C. Wei, and M. J. Cryan, Opt. Express **21**, 27841 (2013).
14. V. V. Klimov, I. V. Zabkov, A. A. Pavlov, R. C. Shiu, H. C. Chan, and G. Y. Guo, Opt. Express **24**, 6172 (2016).
15. W. Huang, Y. Zhang, X. M. Tang, L. S. Cai, J. W. Zhao, L. Zhou, and Y. Y. Zhu, Opt. Lett. **36**, 3359 (2011).
16. W. Zhang, Y. Wang, X. Wen, and Z. Zhang, Appl. Opt. **54**, 9359 (2015).
17. F. Eftekhari and T. J. Davis, Phys. Rev. B **86**, 075428 (2012).
18. T. Fu, Y. Qu, T. Wang, G. Wang, Y. Wang, H. Li, and Z. Zhang, J. Phys. Chem. C **121**, 1299 (2017).
19. X. Yin, M. Schäferling, B. Metzger, and H. Giessen, Nano Lett. **13**, 6238 (2013).
20. T. Narushima, S. Hashiyada, and H. Okamoto, ACS Photon. **1**, 732 (2014).
21. M. Decker, R. Zhao, C. M. Soukoulis, S. Linden, and M. Wegener, Opt. Lett. **35**, 1593 (2010).
22. A. G. Poleshchuk and V. P. Korolkov, Proc. SPIE **6732**, 67320X (2007).
23. S. Vignolini, N. A. Yufa, P. S. Cunha, S. Guldin, I. Rushkin, M. Stefik, and U. Steiner, Adv. Mater. **24**, OP23 (2012).
24. A. Kuzyk, R. Schreiber, Z. Fan, G. Pardatscher, E. M. Roller, A. Högele, and T. Liedl, Nature **483**, 311 (2012).
25. Y. He, G. K. Larsen, W. Ingram, and Y. Zhao, Nano Lett. **14**, 1976 (2014).
26. E. Plum, V. A. Fedotov, and N. I. Zheludev, J. Opt. **13**, 024006 (2010).
27. T. Cao, C. Wei, and L. Zhang, Opt. Mater. Express **4**, 1526 (2014).
28. S. S. Kruk, M. Decker, I. Staude, S. Schlecht, M. Greppmair, D. N. Neshev, and Y. S. Kivshar, ACS Photonics **1**, 1218 (2014).
29. B. Yeom, H. Zhang, H. Zhang, J. I. Park, K. Kim, A. O. Govorov, and N. A. Kotov, Nano Lett. **13**, 5277 (2013).
30. G. K. Larsen, Y. He, W. Ingram, E. T. LaPaquette, J. Wang, and Y. Zhao, Nanoscale **6**, 9467 (2014).
31. Y. Wang, J. Deng, G. Wang, T. Fu, Y. Qu, and Z. Zhang, Opt. Express **24**, 2307 (2016).
32. M. López-García, J. F. Galisteo-López, C. López, and A. García-Martín, Phys. Rev. **85**, 235145 (2012).
33. B. Nordén, *Circular Dichroism and Linear Dichroism* (Oxford University, 1997), Vol. **1**.
34. P. B. Johnson and R. W. Christy, Phys. Rev. B. **6**, 4370 (1972).